Oceanologia (2016) 58, 317—326

Available online at www.sciencedirect.com

ScienceDirect

journal homepage: www.journals.elsevier.com/oceanologia/

ORIGINAL RESEARCH ARTICLE

Performance of operational satellite bio-optical algorithms in different water types in the southeastern Arabian Sea

P. Minu [a], Aneesh A. Lotliker [b], S.S. Shaju [a], P. Muhamed Ashraf [a,*], T. Srinivasa Kumar [b], B. Meenakumari [c]

[a] *ICAR — Central Institute of Fisheries Technology, Kochi, India*
[b] *Indian National Centre for Ocean Information Services (INCOIS), Hyderabad, India*
[c] *Indian Council for Agricultural Research, New Delhi, India*

Received 31 October 2015; accepted 30 May 2016
Available online 16 June 2016

KEYWORDS
Remote sensing reflectance;
Algorithms;
Chlorophyll-*a*;
CDOM;
Arabian Sea;
SATCORE

Summary The *in situ* remote sensing reflectance (R_{rs}) and optically active substances (OAS) measured using hyperspectral radiometer, were used for optical classification of coastal waters in the southeastern Arabian Sea. The spectral R_{rs} showed three distinct water types, that were associated with the variability in OAS such as chlorophyll-*a* (chl-*a*), chromophoric dissolved organic matter (CDOM) and volume scattering function at 650 nm (β_{650}). The water types were classified as Type-I, Type-II and Type-III respectively for the three R_{rs} spectra. The Type-I waters showed the peak R_{rs} in the blue band (470 nm), whereas in the case of Type-II and III waters the peak R_{rs} was at 560 and 570 nm respectively. The shifting of the peak R_{rs} at the longer wavelength was due to an increase in concentration of OAS. Further, we evaluated six bio-optical algorithms (OC3C, OC4O, OC4, OC4E, OC3M and OC4O2) used operationally to retrieve chl-*a* from Coastal Zone Colour Scanner (CZCS), Ocean Colour Temperature Scanner (OCTS), Sea-viewing Wide Field-of-view Sensor (SeaWiFS), MEdium Resolution Imaging Spectrometer (MERIS), Moderate Resolution Imaging Spectroradiometer (MODIS) and Ocean Colour Monitor (OCM2). For chl-*a* concentration greater than 1.0 mg m^{-3}, algorithms based on the reference band ratios 488/510/520 nm to

* Corresponding author at: ICAR — Central Institute of Fisheries Technology, Matsyapuri P.O., Kochi 682029, India. Tel.: +91 4842412300; fax: +91 4842666845.
E-mail address: ashrafp2008@gmail.com (P.M. Ashraf).

Peer review under the responsibility of Institute of Oceanology of the Polish Academy of Sciences.

Production and hosting by Elsevier

http://dx.doi.org/10.1016/j.oceano.2016.05.005

547/550/555/560/565 nm have to be considered. The assessment of algorithms showed better performance of OC3M and OC4. All the algorithms exhibited better performance in Type-I waters. However, the performance was poor in Type-II and Type-III waters which could be attributed to the significant co-variance of chl-*a* with CDOM.

1. Introduction

Ocean colour remote sensing has been widely used as a tool to determine the surface chlorophyll-*a* (chl-*a*) concentration which acts as a proxy for phytoplankton biomass. Several empirical and semi-analytical algorithms have been proposed for the retrieval of chl-*a* from satellite ocean colour data. These algorithms were based on the non-linear relationship between oceanic reflectance and *in situ* measured chl-*a*, more precisely the ratios of reflectance in blue and green bands or their combinations (Lee et al., 2002; O'Reilly et al., 1998, 2000). These algorithms using the spectral ratios of reflectance were mainly attributed to Case 1 waters where the optical properties were determined mainly by phytoplankton and their accessory pigments. For Case 2 waters, apart from phytoplankton, other optically active substances (OAS) such as chromophoric dissolved organic matter (CDOM) and total suspended matter (TSM) contribute significantly to the reflectance (Morel and Prieur, 1977).

The development of ocean chlorophyll 2-band (OC2) and ocean chlorophyll 4-band (OC4) algorithms was done using SeaBAM data set. The OC2 algorithm was revised (OC2 v2) based on an extensive data set of 1174 *in situ* observations and thereafter with the SIMBIOS data set (McClain and Fargion, 1999). O'Reilly et al. (2000) updated OC2 and OC4 with 2853 *in situ* data sets (OC2v2 and OC4v4) and suggested the need to determine accuracy of these revised algorithms in lowest chl-*a* concentrations.

The characteristics of the reflectance spectrum, in terms of shape and magnitude, are largely influenced by the presence of OAS within the water column (Minu et al., 2014; Pierson and Strombeck, 2000). In other words, the apparent optical properties (AOP) of aquatic media, such as remote sensing reflectance (R_{rs}), largely affected by OAS and geometry of ambient light field can be quantified using inherent optical properties (IOPs) of the OAS (Mobley, 1994; Morel, 1991). The fundamental IOPs influencing the R_{rs} are absorption (a), scattering (b) and volume scattering function (β). The phytoplankton pigment, chl-*a*, has a tendency to absorb light in the blue and red bands of the visible electromagnetic spectrum (V-EMS) with the former being the primary peak. The CDOM also exhibits strong absorption in UV and the shorter wavelength band of V-EMS whereas the suspended matter usually scatters in the longer wavelength band. Apart from this, the water molecules themselves absorb strongly in the red part of V-EMS. Further, the volume scattering describes the angular distribution of light scattered from an incident beam. In the absence of inelastic scattering, IOP of a medium is completely determined by the absorption coefficient and β. These when combined with the angular and spectral distribution of the incident radiance field, just below the surface, the full radiative flux balance of the ocean can be simulated (Lee and Lewis, 2003). Studies using hyperspectral radiometers, on the relationship between IOP and concentration of OAS, indicated the presence of identifiable sub-types of coastal water within the conventional Case 2 classification (Mckee and Cunningham, 2006).

The ratio based empirical algorithms for the retrieval of chl-*a* from CZCS, MOS-B, IRS-P4-OCM and SeaWiFS have been already carried out in the southeastern Arabian Sea. Sathe and Jadhav (2001) studied retrieval of chl-*a* using sea-leaving radiance from MOS-B and showed that the single ratio of CZCS algorithm fails in the Arabian Sea. They also reported that the two factor algorithm of SeaWIFS fails in 30% of the cases. Further, Nagamani et al. (2008) reported that OC4v4 algorithm overestimates chl-*a* in the northern Arabian Sea when compared to MBR based OCM-2 algorithm. In addition to these, Chauhan et al. (2002) evaluated the accuracy, precision and suitability of different ocean colour algorithms for the Arabian Sea. According to their study, OC2 and OC4 algorithms performed well in Case 1 waters of the Arabian Sea. But both algorithms failed to estimate chlorophyll in *Trichodesmium* dominated waters. Tilstone et al. (2011) also assessed three algorithms, OC4v6, Carder and OC5, for retrieving chl-*a* in coastal areas of the Bay of Bengal and open ocean areas of the Arabian Sea. Based on the accuracy assessment, they recommended the use of the OC5 algorithm in the area of study. Most of these studies were confined to oligotrophic to mesotrophic waters. Assessment of MODIS-aqua chlorophyll-*a* algorithms in coastal and shelf waters of the southeastern Arabian Sea showed better performance of OC3M than GSM and GIOP (Tilstone et al., 2013). However, our study deals with mesotrophic to eutrophic waters. The problem with estimating chl-*a* from an ocean colour satellite sensor involves two critical steps. The first step is to eliminate the effect of the atmospheric contribution and the second step is to select a suitable bio-optical algorithm. In this study, we have focused on *in situ* bio-optical data, measured using hyperspectral radiometer, in the optically complex waters of the southeastern Arabian Sea, with the following objectives:

1. Analyzing the spectral remote sensing reflectance in the view of distribution of OAS.
2. Evaluation of operational empirical algorithm in different water types.

2. Study area

A part of the southeastern Arabian Sea forms the study area (Fig. 1). The area has a strong monsoonal influence resulting

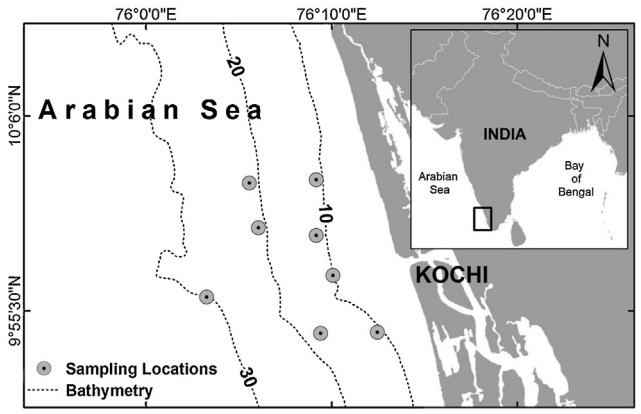

Figure 1 Map of study area showing the sampling stations.

in seasonal changes in hydrographic conditions influenced by river water discharge and surface circulation. During pre-monsoon season (February–May) wind-induced upwelling along with a northward undercurrent and a southward surface flow associated with strong vertical mixing are observed off Kochi waters (Kumar and Kumar, 1996). During the monsoon period, freshwater discharge from adjoining rivers increases the nutrient concentrations of the coastal waters along with the detrital load. These rapid changes often lead to very high production at primary and secondary levels (George et al., 2013). Upwelling process supported by the southerly current is also observed along the coastal waters during monsoon season (Joshi and Rao, 2012). The previous studies reported that freshwater discharge from the estuary and the high organic load of the bottom sediment are the potential factors affecting the biogeochemistry of the study area (Iyer et al., 2003; Srinivas and Dineshkumar, 2006).

3. Material and methods

3.1. *In situ* data

The data used for the present study was generated as a part of SATellite Coastal and Oceanographic REsearch (SATCORE) programme coordinated by Indian National Centre for Ocean Information Services (INCOIS). The data was generated, with monthly frequency, from eight stations, between April 2009 and 2011. The sampling was carried out using commercial purse seiner. Satlantic™ hyperspectral radiometer (HyperOCRII) was operated in all the stations. The instrument contains optical sensors which measure downwelling surface irradiance (E_s) and profiles of upwelling radiance (L_u) and downwelling irradiance (E_d). Apart from these the ancillary sensors measures tilt, pressure, temperature and conductivity. The radiometer was also equipped with ECO triplet sensor (Wetlabs™ ECO series) which measures chlorophyll fluorescence, CDOM fluorescence and β at 650 nm (β_{650}). The excitation and emission wavelengths to measure CDOM fluorescence were 370 and 460 nm respectively with a sensitivity of 0.28 ppb of quinine sulphate dihydrate equivalent (QSDE). The volume scattering function, β, when integrated in backward direction provides estimates of backscattering (Balch et al., 2001). The backscattering at longer wavelengths, especially in red, is more sensitive to the suspended matter. Hence in the present study β is considered as a measure of total suspended matter.

Utmost care was taken to avoid tilt, maintain profiling velocity and avoid shadows from sources. The data from hyperspectral radiometer was recorded using SatView™ software and multi-level processing was carried out using Prosoft™ software.

The spectral R_{rs} was computed as

$$R_{rs}(0^+,\lambda) = \frac{L_w(0^+,\lambda)}{E_d(0^+,\lambda)}, \quad (1)$$

where $L_w(0^+, \lambda)$ is water leaving radiance and $E_d(0^+, \lambda)$ is downwelling irradiance above the sea surface. Further the upwelling radiance and downwelling radiance were computed as follows:

$$E_d(0^+,\lambda) = \frac{E_d(0^-,\lambda)}{1-\alpha}, \quad (2)$$

where α is the Fresnel reflection albedo for irradiance from the sun and sky and

$$L_w(0^+,\lambda) = L_u(0^-,\lambda)\frac{[1-\rho(\lambda,\theta)]}{\eta_w^2(\lambda)}, \quad (3)$$

where $\rho(\lambda, \theta)$ is the Fresnel reflectance index of seawater and $\eta_w(\lambda)$ is the Fresnel refractive index of seawater.

The spectral R_{rs}, measured using radiometer, was then used as an input to derive the chlorophyll concentration from respective algorithms.

3.2. Empirical algorithms

Six operational empirical algorithms (OC3C, OC4O, OC4, OC4E, OC3M, OC4O2) were selected for this study. These algorithms have been operationally implemented as default algorithms for Costal Zone Colour Scanner (CZCS), Ocean Colour and Temperature Scanner (OCTS), Sea-viewing Wide Field-of-view Sensor (SeaWiFS), Medium Resolution Imaging Spectrometer (MERIS), Moderate Resolution Imaging Spectroradiometer (MODIS) and Ocean Colour Monitor (OCM2). The functional forms of these algorithms are given in Table 1.

These algorithms have undergone several revisions based on the *in situ* data generated from different water types. The OC2 algorithm, originally designed for CZCS, has undergone eight revisions (OC2a, OC2b, OC2c, OC2d, OC2e, OC2, OC2v2 and OC2v4). The latest of which is OC2v4 which has a modified cubic polynomial form. The OC4O algorithm, designed for OCTS, has undergone four revisions and emerged as 4th order polynomial function relating the maximum of three band ratios. The OC4 algorithm, designed for SeaWiFS, has two versions (OC4 and OC4v4). Both versions use maximum ratio of four bands. The first version of OC4 was a modified cubic polynomial and the current version uses a fourth order polynomial with five coefficients (O'Reilly et al., 1998, 2000). The OC4E algorithm, designed for MERIS, is the tuned version of OC4v4 and has the functional form of 4th order cubic polynomial. The OC3 algorithm, designed for MODIS had undergone two versions (OC3d, and OC3e). It is three banded maximum band ratio and uses fourth order polynomial function. The default algorithm for OCM-2 is third order modified cubic polynomial which used the maximum ratio of four bands (Nagamani et al., 2008).

Table 1 The functional forms of the algorithms used to generate chl-*a* from Coastal Zone Colour Scanner (CZCS), Ocean Colour and Temperature Scanner (OCTS), Sea-viewing Wide Field-of-view Sensor (SeaWiFS), Medium Resolution Imaging Spectrometer (MERIS), Moderate Resolution Imaging Spectroradiometer (MODIS) and Ocean Colour Monitor 2 (OC4O2).

Sensor	Algorithm	Functional form	Model type
CZCS	OC3C MBR	$R = \log_{10}\left\{\max\left[\left(\frac{R_{rs}443}{R_{rs}550}\right), \left(\frac{R_{rs}520}{R_{rs}550}\right)\right]\right\}$ $a = [0.3330, -4.3770, 7.6267, -7.1457, 1.6673]$ $C = 10^{(a_0+a_1R+a_2R^2+a_3R^3+a_4R^4)}$	Fourth order polynomial
OCTS	OC4O MBR	$R = \log_{10}\left\{\max\left[\left(\frac{R_{rs}443}{R_{rs}565}\right), \left(\frac{R_{rs}490}{R_{rs}565}\right), \left(\frac{R_{rs}520}{R_{rs}565}\right)\right]\right\}$ $a = [0.2399, -2.0825, 1.6126, -1.0848, -0.2083]$ $C = 10^{(a_0+a_1R+a_2R^2+a_3R^3+a_4R^4)}$	Fourth order polynomial
SeaWiFS	OC4 MBR	$R = \log_{10}\left\{\max\left[\left(\frac{R_{rs}443}{R_{rs}555}\right), \left(\frac{R_{rs}490}{R_{rs}555}\right), \left(\frac{R_{rs}510}{R_{rs}555}\right)\right]\right\}$ $a = [0.2515, -2.3798, 1.5823, -0.6372, -0.5692]$ $C = 10^{(a_0+a_1R+a_2R^2+a_3R^3+a_4R^4)}$	Fourth order polynomial
MERIS	OC4E MBR	$R = \log_{10}\left\{\max\left[\left(\frac{R_{rs}443}{R_{rs}560}\right), \left(\frac{R_{rs}490}{R_{rs}560}\right), \left(\frac{R_{rs}510}{R_{rs}560}\right)\right]\right\}$ $a = [0.2521, -2.2146, 1.5193, -0.7702, -0.4291]$ $C = 10^{(a_0+a_1R+a_2R^2+a_3R^3+a_4R^4)}$	Fourth order polynomial
MODIS	OC3M MBR	$R = \log_{10}\left\{\max\left[\left(\frac{R_{rs}443}{R_{rs}547}\right), \left(\frac{R_{rs}488}{R_{rs}547}\right)\right]\right\}$ $a = [0.2424, -2.7423, 1.8017, -0.0015, -1.2280]$ $C = 10^{(a_0+a_1R+a_2R^2+a_3R^3+a_4R^4)}$	Fourth order polynomial
OCM2	OC4O2 MBR	$R = \log_{10}\left\{\max\left[\left(\frac{R_{rs}443}{R_{rs}555}\right), \left(\frac{R_{rs}490}{R_{rs}555}\right), \left(\frac{R_{rs}510}{R_{rs}555}\right)\right]\right\}$ $a = [0.475, -3.029, 2.240, -1.253, -0.027]$ $C = 10^{(a_0+a_1R+a_2R^2+a_3R^3+a_4R^4)}$	Third order modified cubic polynomial

4. Results

The results of the present study have been described in the following three sections. The first section deals with the optical classification of coastal waters based on AOP. The second section deals with the association of OAS with spectral R_{rs} and the third section with the assessment of ocean colour algorithms in different water types.

4.1. Optical classification using remote sensing reflectance

The entire data sets exhibited three different types of R_{rs} spectra and their spectral variability is given in Fig. 2. Based on the variability in R_{rs} spectra, the coastal waters off Kochi are optically classified into three types. Type-I waters had spectra (Fig. 2a) with flatter curve between 400 and 450 nm which then increased to peak at 482 nm. After 482 nm, R_{rs} decreased gradually till 608 nm and then the curve flattened again till 700 nm indicating no reflectance in the region. The spectral R_{rs} in Type-II waters (Fig. 2b) was found to be distinct from that of Type-I. The average R_{rs} increased gradually from shorter wavelength (400 nm) and showed almost a flat peak between 532 and 566 nm with a marginally higher value at 560 nm. Beyond 560 nm, a steep valley was observed till 610 nm. After which the decrease was gradual till 670 nm. A secondary maximum was also observed at 681 nm. The R_{rs} spectra in Type-III waters (Fig. 2c) showed similarity to that of the Type-II at the longer wavelength. In this type, a steep increase in R_{rs} was observed from 400 to 570 nm. The peak R_{rs} was more prominent. The spectral behaviour of R_{rs} from 570 to 700 nm in this water type was similar to that of Type-II. However, the secondary maximum was more prominent (684 nm) and higher in magnitude.

4.2. Association of optically active substances with different water types

The analyses of spatio-temporal variability in OAS (chl-*a* and CDOM) and their IOP (β_{650}) have been carried out for the

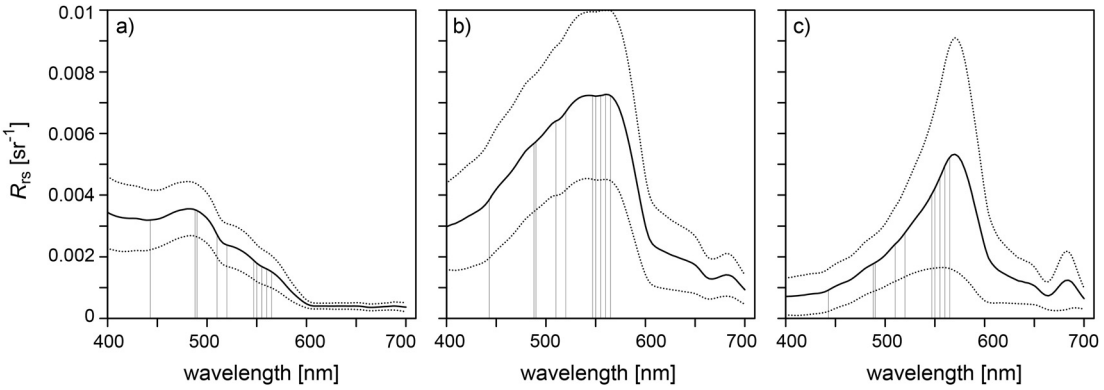

Figure 2 Spectral variability of remote sensing reflectance (R_{rs}) in the study area. The similar spectra have been clubbed together as (a) Type-I, (b) Type-II and (c) Type-III. The solid line represent mean and the dotted line represents the standard deviation. The *X*-axis represents wavelength [nm] and *Y*-axis represents R_{rs} [sr^{-1}] coefficients.

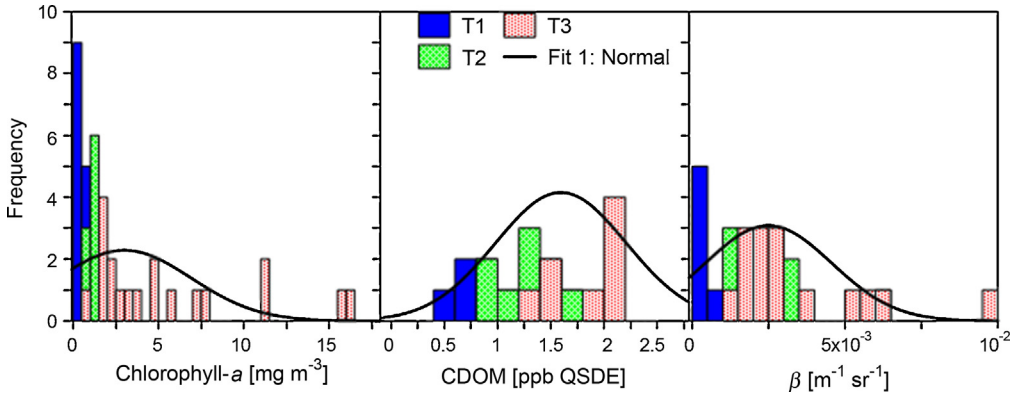

Figure 3 Frequency distribution of chlorophyll-*a* (chl-*a*), volume scattering function at 650 nm (β_{650}) and concentration of chromophoric dissolved organic matter (CDOM) in quinine sulphate dihydrate equivalent (QSDE) unit in different water types. The solid line indicates the normal distribution. The *X*-axis represents concentration of chl-*a*, β_{650} and CDOM. The *Y*-axis represents frquency distribution.

three water types based on the frequency distribution (Fig. 3). The frequency distribution plots were also superimposed with the normal Gaussian function to understand the trend. The frequency distribution showed large variability in the OAS for the three water types. The chl-*a*, which varied between the three water types, was 0.077 and 20.0 mg m^{-3} (Fig. 3a). The chl-*a* in Type-I and Type-II waters ranged from 0.77 to 1.0 mg m^{-3} and 1.0 and 2.0 mg m^{-3} respectively. The Type-III waters, chl-*a* ranged from 1 to 20 mg m^{-3} while the frequency was less at lower concentration.

The CDOM varied between 0.39 and 2.25 ppb QSDE (Fig. 3b). Type-I waters showed lower concentration of CDOM, between 0.3 and 0.75 ppb QSDE. The CDOM concentration in Type-II and Type-III waters are varied, from 0.75 to 1.25 and Hp1.25 to 2.25 ppb QSDE respectively. The concentration of CDOM was comparatively higher in Type-II waters. β_{650}, ranged between 0.16×10^{-3} and 9.5×10^{-3} m^{-1} sr^{-1} (Fig. 3c) with a higher frequency at the lower range between 0.16×10^{-3} and 0.19×10^{-3} m^{-1} sr^{-1}. In Type-II and Type-III waters, β_{650} was in the range from 1.3×10^{-3} to 6.1×10^{-3} m^{-1} sr^{-1} and 1.4×10^{-3} to 9.5×10^{-3} m^{-1} sr^{-1} respectively. The maximum value of β_{650} was encountered in Type-III waters.

4.3. Assessment of ocean chlorophyll algorithms

The scatter plots showing relation between *in situ* measured chl-*a* and that derived using OC4, OC3C, OC4O, OC4E, OC3M and OC4O2 algorithms is given in Fig. 4. The validation statistics have been computed using data from all water types. The corresponding statistical indicators are given in Table 2. The R^2 was better in case of OC4 (0.70), which was also comparable with that of OC3M (0.68). Further OC4 and OC3M showed least Log_{10}-RMSE (0.37). However, absolute percentage difference (APD) (35.9%) was better in case of OC4 whereas OC3M showed better slope (0.69), relative percentage difference (RPD) (4.8%) and unbiased percentage difference (UPD) (17.1%). The intercept (0.07) was least in the case of OC4O and '*r*' was closer to unity in case of OC4O2. The inverse transform ratios also showed that OC3M performs better at the median scale with F_{med} close to unity. The overall statistical analysis showed that OC3M and OC4 produced comparable results having least significant difference between estimated and measured chl-*a*.

Although the validation has been carried out for the entire data set, the accuracy of the algorithms was also evaluated in the different water types. The assessment of measured and

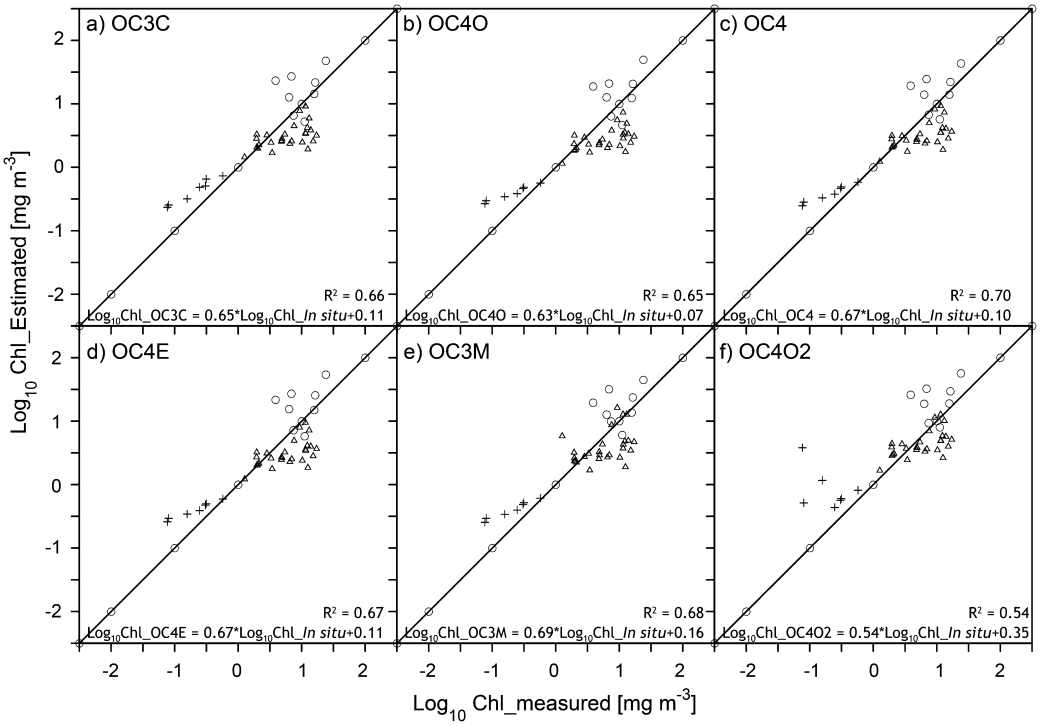

Figure 4 Correlation between *in situ* chlorophyll-*a* (chl-*a*) and that derived using OC4, OC3C, OC4O, OC4E, OC3M and OC4O2 algorithms in Type-I (plus), II (triangle) and III (circle) waters. The solid line indicate the trend and the dotted line corresponds to 1:1.

Table 2 Performance indices for relative errors between *in situ* measured and estimated chl-*a* from *in situ* R_{rs} using OC3C, OC4O, OC4, OC4E, OC3M and OC4O2 algorithms. These indices include correlation coefficient (R^2), slope (S), intercept (I), sumation of ratio of measured to estimated (r), root mean squared error (RMSE), absolute percentage difference (APD), relative percentage difference (RPD) and unbiased percentage difference (UPD). The geometric mean and one-sigma range of the ratio (F = $Value_{alg}/Value_{meas}$) are given by F_{med}, F_{min}, and F_{max}, respectively. The values closer to 1 are more accurate. Total 42 data points were used for the analysis.

Algorithm	R^2	S	I	r	RMSE	APD	RPD	UPD	F_{min}	F_{med}	F_{max}
OC3C	0.66	0.65	0.11	1.74	0.39	41.0	17.2	29.8	0.50	1.21	2.94
OC4O	0.65	0.63	**0.07**	1.95	0.41	40.3	23.6	36.5	**0.56**	1.36	3.34
OC4	**0.70**	0.67	0.10	1.69	**0.37**	**35.9**	16.3	26.7	0.53	1.22	2.82
OC4E	0.67	0.67	0.10	1.70	0.38	37.2	16.6	27.7	0.50	1.20	2.88
OC3M	0.68	**0.69**	0.16	1.47	**0.37**	50.4	**4.8**	**17.1**	0.44	**1.04**	2.45
OC4O2	0.54	0.54	0.35	**1.21**	0.45	47.1	3.26	30.1	0.29	0.82	2.29

estimated chl-*a* in Type-I waters showed a good agreement with a correlation coefficient (R^2) of 0.93 in the case of OC4O, OC4, OC4E and OC3M and 0.89 in the case of OC3C. Chl-*a* estimated using OC4O2 algorithm showed relatively lower correlation (R^2 = 0.74). However, the measured chl-*a* was lower in magnitude than the estimated chl-*a* having a slope of 1.06, 0.60, 0.68, 0.67, 0.71 and 0.68 for OC3C, OC4O, OC4, OC4E, OC3M and OC4O2 respectively. The result based on the statistical analysis indicated that OC3M performs better than other algorithms in Type-I waters. In Type-II waters, it was observed that a cluster of points having chl-*a* concentration between 9.0 and 13 mg m^{-3} showed a poor relation between estimated and measured chl-*a*. At these points, β_{650} was ten-fold higher than that in Type-I waters. In addition, the CDOM was higher than the average value (2.1—2.5 ppb QSDE). In the absence of this cluster, it was observed that estimated and measured chl-*a* had moderate agreement in case of OC3C (R^2 = 0.52), OC4 (R^2 = 0.67), OC4E (R^2 = 0.67), OC3M (R^2 = 0.67) and OC4O2 (R^2 = 0.67). In this water type, estimated chl-*a* was lower in magnitude than the measured with a slope of 0.59, 0.50, 0.63, 0.63, 0.90 and 0.88 for OC3C, OC4O, OC4, OC4E, OC3M and OC4O2 respectively. Based on the statistical analysis, comparable result was seen between OC3M and OC4O2. The performance of both these algorithms was better than other algorithms in Type-II waters. In Type-III waters, estimated chl-*a* was found to be higher in magnitude as compared to measured chl-*a*. The slope of regression was 1.46, 1.45, 1.39, 1.65, 1.44 and 1.84 for OC3C, OC4O, OC4, OC4E, OC3M and OC4O2 respectively. Although the estimated and measured chl-*a* was found to be variable in magnitude, the trend was in good agreement. The R^2 was 0.68, 0.63, 0.69, 0.66, 0.70 and 0.70 for OC3C, OC4O, OC4, OC4E, OC3M and OC4O2 respectively. The OC3M and OC4 algorithms performed better in Type-III waters.

An attempt has been also made to understand existence of any covariance between CDOM and errors associated with the

algorithms in Type-II and III waters. Hence a ratio of estimated chl-*a*, from various algorithms, to *in situ* chl-*a* was regressed with CDOM. The results showed that in Type-II waters, the covariance was 2.48, 1.42, 2.24, 2.48, 5.16 and 2.99% whereas in Type-III it was 39.64, 25.96, 27.09, 30.46, 25.41 and 35.86% respectively for OC3C, OC4O, OC4, OC4E, OC3M and OC4O2 algorithms.

5. Discussion

The retrieval of geophysical products from an ocean colour satellite sensor involves two critical steps. The first step is to eliminate the effect of the atmospheric contribution from the total radiance received by the satellite sensor (Hu et al., 2004). The second step is to select a suitable bio-optical algorithm which relates the signal leaving the water column with the concentration of the OAS. The present study aims towards the second step. In the present case, the empirical algorithms, used operationally to retrieve chl-*a* from CZCS, OCTS, SeaWiFS, MERIS, MODIS and OCM2, were applied to the *in situ* R_{rs} measured using hyperspectral radiometer. Further, an attempt has been also made to classify the waters based on the reflectance characteristics and to evaluate impact of OAS on these water types. Subsequently the performance of these algorithms was tested in these water types.

The data generated for the present study exhibited three distinct spectra for R_{rs}. The distribution of OAS within different water types also showed a remarkable difference. In Type-I waters, R_{rs} spectra showed the maximum in the blue (400–480 nm) region and was almost negligible in the red region (beyond 600 nm). The variability in concentration of chl-*a* and CDOM was very low in this water type with a standard deviation of less than 50% of the average value. The β_{650} also showed less variability in this water type. The low concentration in distribution of OAS in Type-I waters was responsible for least absorption in the shorter wavelength resulting in high R_{rs}. However, the lower R_{rs} in the longer wavelength may be attributed to the strong absorption due to water molecules. This indicates that the water molecules were the principal light absorbing component in this water type along with chl-*a*. This is in agreement with the previous studies carried out in oligotrophic waters of Lakshadweep Islands, hyperoligotrophic waters in the South Pacific gyre and in the Chesapeake Bay where the authors have shown that the water molecules are the major components responsible for the absorption in the longer wavelength resulting in minimal variability of R_{rs} (Menon et al., 2005; Morel et al., 2007; Tzortziou et al., 2007). The spectral signature of R_{rs} in Type-II waters showed significant difference in shorter wavelengths. In Type-II waters, chl-*a* concentration and β_{650} was ten-fold higher than in Type-I waters. Also, the CDOM concentration was almost twice in magnitude. The phytoplankton pigment, chl-*a*, has the primary absorption peak in the blue region (~440 nm). Apart from this, CDOM also has a tendency for strong absorption in UV and the blue region (Jorgenson, 1999; Menon et al., 2005; Siegal et al., 2002). Therefore, the respective signature of R_{rs} in Type-II waters was predominantly due to the combined effect of absorption due to chl-*a* and CDOM. In Type-III waters, the peak in the R_{rs} spectra shifted more towards the longer wavelength as compared to that in Type-II waters. In addition, the peak R_{rs} was more prominent as compared to Type-I and II waters. In this water type, β_{650} was comparable with Type-II waters. However, chl-*a* and CDOM concentration was found to be increased by 64% and 76% respectively. This indicates that the impact of chl-*a* and CDOM absorption has further increased which resulted in much lower R_{rs} at the shorter wavelength. Menon et al. (2006) showed that CDOM significantly influences the water leaving radiance at the shorter wavelengths and its impact can be spread up to 650 nm. Kutser et al. (2006) reported an 'abnormal' shape of the R_{rs} spectra when the concentrations of optically active substances were high. The study carried out by Cannizaro and Carder showed that, in non-coastal oligotrophic waters, the peak R_{rs} was at 400 nm which was shifted to ~490 nm in highly reflective, optically shallow, mesotrophic waters and ~560 nm in optically deep eutrophic waters. Ouillon and Petrenko (2005) also reported peak R_{rs} at 443 and 490 nm in Case 1 waters and at 560 nm in Case 2 waters.

The above discussion clearly indicates that distinct spectral signatures of R_{rs} were more attributed towards variability in OAS. Further, the distribution of these OAS could be controlled by hydrography of the study area. The study area is subjected to coastal upwelling and heavy fresh water discharge from the estuary of the Periyar River in the monsoon period which enhances nutrient upload resulting in increased biological production (Jyothibabu et al., 2006; Nair et al., 1992). Studies by Srinivas et al. (2003) also reported that the coastal waters of the southeastern Arabian Sea are the recipient of approximately 1.9×10^{10} m^3 of fresh water annually from the Cochin backwaters. We have also analyzed the inter-relationship of chl-*a* with CDOM and β_{650} in different water types (Fig. 5). The chl-*a* and CDOM did not show any significant relation in Type-I waters. This indicates that CDOM is independent of the variations in chl-*a* in these waters. However a large association was seen in Type-II and Type-III waters. Also in these waters, the concentration of chl-*a* and CDOM was very high. The co-variance of chl-*a* with CDOM indicates that the source of nutrients for phytoplankton growth, and organic matter is the same. Since the primary source of CDOM is from the river, it can be inferred that river discharges are one of the primary mechanisms for distribution of chl-*a* and CDOM in the study area. The β_{650} did not show any significant relationship with chl-*a* in any of the water types. This indicates that chl-*a* and suspended matter do not co-vary in water types. Hence, it can be inferred that river discharges are not the primary source of suspended matter in the study area. Some of the previous studies by Jyothibabu et al. (2006), Srinivas et al. (2003) and Thomas et al. (2004) also reported that continuous dredging process occurring throughout the year in the study area increases the nutrients and sediment loads into the estuary which is drained into the coastal waters.

The distribution of OAS thus significantly alters the spectral R_{rs} which is the input for the empirical algorithm for the retrieval of chl-*a*. In the present study, chl-*a* algorithms were evaluated in different water types having similar variability in spectral R_{rs}. Among all the algorithms, OC3M and OC4 performed better in the study area. In general, all algorithms showed that, in Type-I waters, the measured chl-*a* was less than that estimated using various algorithms. However measured and estimated chl-*a* showed the same trend with good correlation. These waters were having typical Case 1 characteristics. Also the R_{rs} signals dominated in 443 nm band. In

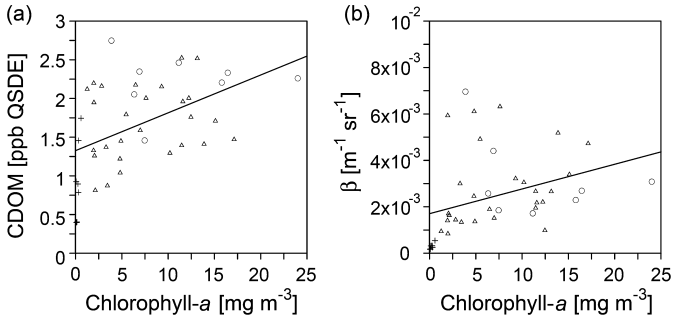

Figure 5 Scatter plot showing relation between (a) *in situ* chlorophyll-*a* (chl-*a*) and CDOM in QSDE unit and (b) *in situ* chl-*a* and β. The plus (+) sign corresponds to Type-I, open triangle (△) corresponds to Type-II and open circles (○) corresponds to Type-III waters.

Type-II waters, the cluster of points was found to be weakly correlated. Further in Type-II waters, the dominant signal in R_{rs} was from the blue-green band. In the case of OC4, OC4E and OC4O2 the dominant R_{rs} signal was from 510 nm, whereas it was 520 nm in the case of OC3C and OC4O. For OC3M, R_{rs} signal was dominated by the 488 nm band. Similar conditions were observed in Type-III waters. The performance of all the algorithms was poor in Type-II waters whereas it was comparatively better in Type-III waters. Although in Type-II and Type-III waters concentration of chl-*a* and CDOM was ten-fold higher than Type-I waters, the co-variance between chl-*a* and CDOM was significantly higher in Type-III waters. Desa et al. (2001) showed that the ratio of R_{rs} at 490—555 nm is a better indicator of chl-*a* in the eastern Arabian Sea. They illustrated significant improvement in R^2 (0.93), slope (0.96) and intercept (0.26) by modifying SeaWiFS OC4v4 coefficients. However Shanmugam (2011) suggested that although OC3 reliably estimates chl-*a* in the open ocean waters, it tends to fail in the coastal waters of the Arabian Sea. The chl-*a* and CDOM compete for absorption of light at almost similar wavelengths in the blue region. As a result, the signal emerging from the water column carries signatures of both chl-*a* and CDOM. The empirical algorithms take the ratio of the blue to the green band with an assumption that the water leaving radiance decreases in the blue band with an increase in chl-*a* concentration. However, if the water column is dominated by chl-*a* and CDOM, both significantly contribute to the decrease in the water leaving radiance in the blue band. In such a scenario, the performance of a ratio based algorithms weakens the retrieval of chl-*a*. In the earlier studies, Tzortziou et al. (2007) also reported that the failure of MODIS algorithm in inshore waters of the Chesapeake Bay was due to the large contribution of non-co-varying CDOM and non-algal particles to total light absorption in the blue region.

6. Conclusion

The present study primarily focused on the evaluation of six empirical algorithms (OC3C, OC4O, OC4, OC4E, OC3M and OC4O2), operationally used to retrieve chl-*a* from CZCS, OCTS, SeaWiFS, MERIS, MODIS and OCM-2. The algorithms were applied to the spectral R_{rs} measured *in situ* using hyperspectral radiometer with an intention to assess the functional form and the coefficients. The effect of atmospheric correction has been ignored in the present study. The R_{rs} showed three distinct water types based on the spectral variability. These water types were attributed to the variability in the concentration of OAS. In Type-I waters chl-*a*, CDOM and β_{650} were very low indicating that these were pure Case-I waters and the peak R_{rs} was in the blue band. In Type-II waters, the peak R_{rs} shifted to the green band which was attributed to elevated concentration of chl-*a*, CDOM and β_{650}. In Type-III waters, the peak R_{rs} further shifted to longer wavelengths due to an increase in chl-*a* and CDOM. Also chl-*a* was found to be associated with CDOM indicating that rivers are one of the primary sources for discharging essential parameters for the growth of phytoplankton. The overall statistical analysis showed that the performances of OC3M and OC4 were better as compared to other algorithms. Further in the case of chl-*a*, at more than 1.0 mg m^{-3} it was found that the ratio of higher wavelengths (488, 510 and 520 nm) dominates. The assessment of algorithms in different water types indicated better performance of all the algorithms in Type-I waters. The performance was poor in Type-II and Type-III waters. The errors associated with the estimation of chl-*a* were significantly co-varied with CDOM in Type-III waters. Therefore, in the regions where there is dominance of OAS other than chl-*a*, it is required to develop IOP-based algorithm that takes into account absorption and scattering due to individual OAS.

Acknowledgements

The study was funded by Indian National Centre for Ocean Information Services (INCOIS) (INCOIS:F&A:XII:D2:021), Ministry of Earth Sciences under SATellite Coastal Oceanographic REsearch (SATCORE) programme. The authors are thankful to the Director of INCOIS for encouragement. Thanks are also due to the Director of ICAR — Central Institute of Fisheries Technology, for support and encouragement. The authors are also grateful to the management and staff of MV 'Bharath Darshan', for their unrestricted support during the cruises.

References

Balch, W.M., Drapeau, D., Fritz, J., Bowler, B., Nolan, J., 2001. Optical backscattering in the Arabian Sea — continuous underway measurements of particulate inorganic and organic carbon. Deep-Sea Res. Pt. I 48 (11), 2423—2452, http://dx.doi.org/10.1016/S0967-0637(01)00025-5.

Chauhan, P., Mohan, M., Sarangi, R.K., Kumari, B., Nayak, S., Matondkar, S.G.P., 2002. Surface chlorophyll estimation in the Arabian Sea using IRS-P4 OCM Ocean Color Monitor (OCM) satellite data. Int. J. Remote Sens. 23 (8), 1663–1676, http://dx.doi.org/10.1080/01431160110075866.

Desa, E.S., Suresh, T., Matondkar, S.G.P., Desa, E., 2001. Sea truth validation of SeaWiFS ocean colour sensor in the coastal waters of the eastern Arabian Sea. Curr. Sci. India 80 (7), 854–860.

George, R., Muraleedharan, K.R., Martin, G.D., Sabu, P., Gerson, V. J., Dineshkumar, P.K., Nair, S.M., Chandramohanakumar, N., Nair, K.K.C., 2013. Nutrient biogeochemistry of the eastern Arabian Sea during the southwest monsoon retreat. Environ. Earth Sci. 68 (3), 703–718, http://dx.doi.org/10.1007/s12665-012-1772-2.

Hu, C., Montgomery, E.T., Schmitt, R.W., Muller-Karger, F.E., 2004. The dispersal of the Amazon and Orinoco River water in the tropical Atlantic and Caribbean Sea: observation from space and S-PALACE floats. Deep-Sea Res. Pt. II 51 (10–11), 1151–1171, http://dx.doi.org/10.1016/j.dsr2.2004.04.001.

Iyer, P.C.S., Sindhu, M., Kulkarni, S.G., Tambe, S.S., Kulkarni, B.D., 2003. Statistical analysis of the physic-chemical data on the coastal waters of Cochin. J. Environ. Monitor. 5 (2), 324–327, http://dx.doi.org/10.1039/B209219K.

Jorgenson, S.V., 1999. Standard Case 1 algorithms in Danish coastal waters. Int. J. Remote Sens. 20 (7), 1289–1301, http://dx.doi.org/10.1080/014311699212731.

Joshi, M., Rao, A.D., 2012. Response of Southwest monsoon winds on shelf circulation off Kerala coast, India. Cont. Shelf Res. 32, 62–70, http://dx.doi.org/10.1016/j.csr.2011.10.015.

Jyothibabu, R., Madhu, N.V., Jayalakshmi, K.V., Balachandran, K.K., Shiyas, C.A., Martin, G.D., Nair, K.K.C., 2006. Impact of fresh water influx on microzooplankton mediated food web in a tropical estuary (Cochin backwaters – India). Estuar. Coast. Shelf Sci. 69 (3–4), 505–518, http://dx.doi.org/10.1016/j.ecss.2006.05.013.

Kumar, H.P.V., Kumar, M.N., 1996. On the flow and thermohaline structure off Cochin during pre-monsoon season. Cont. Shelf Res. 16 (4), 457–468, http://dx.doi.org/10.1016/j.ecss.2006.05.013.

Kutser, T., Vahtma, E., Martin, G., 2006. Assessing suitability of multispectral satellites for mapping benthic macroalgal cover in turbid coastal waters by means of model simulations. Estuar. Coast. Shelf Sci. 67 (3), 521–529, http://dx.doi.org/10.1016/j.ecss.2005.12.004.

Lee, M.E., Lewis, M.R., 2003. A new method for the measurement of the optical volume scattering function in the upper ocean. J. Atmos. Ocean. Tech. 20 (4), 563–571, http://dx.doi.org/10.1175/1520-0426(2003)20<563:ANMFTM>2.0.CO;2.

Lee, Z., Carder, K.L., Arnone, R.A., 2002. Deriving inherent optical properties from water color: a multiband quasi-analytical algorithm for optically deep waters. Appl. Opt. 41 (27), 5755–5772, http://dx.doi.org/10.1364/AO.41.005755.

McClain, M.E., Fargion, G.S., 1999. Simbios project annual report. Document ID: 20000013962, Report/Patent Number: NASA/TM-1999-209486, NAS 1.15:209486 Rept-2000-00655. Goddard Space Flight Center, Greenbelt, Maryland, 132 pp.

Mckee, D., Cunningham, A., 2006. Identification and characterization of two optical water types in the Irish Sea from in situ inherent optical properties and seawater constituents. Estuar. Coast. Shelf Sci. 68 (1), 305–316, http://dx.doi.org/10.1016/j.ecss.2006.02.010.

Menon, H.B., Lotliker, A.A., Moorthy, K.K., Nayak, S.R., 2006. Variability of remote sensing reflectance and implications for optical remote sensing – a study along the eastern and northeastern waters of Arabian Sea. Geophys. Res. Lett. 33, L15602, http://dx.doi.org/10.1029/2006GL026026.

Menon, H.B., Lotliker, A.A., Nayak, S.R., 2005. Pre-monsoon bio-optical properties in estuarine, coastal and Lakshadweep waters. Estuar. Coast. Shelf Sci. 63 (1), 211–223, http://dx.doi.org/10.1016/j.ecss.2004.11.015.

Minu, P., Lotliker, A.A., Shaju, S.S., SanthoshKumar, B., Ashraf, P.M., Meenakumari, B., 2014. Effect of optically active substances and atmospheric correction schemes on remote-sensing reflectance at a coastal site off Kochi. Int. J. Remote Sens. 35 (14), 5434–5447, http://dx.doi.org/10.1080/01431161.2014.926420.

Mobley, C.D., 1994. The optical properties of water. In: Bass, M. (Ed.), Handbook of Optics, 2nd ed., vol. I. McGraw-Hill, New York, 1248 pp.

Morel, A., 1991. Light and marine photosynthesis: a spectral model with geo-chemical and climatological implications. Prog. Oceanogr. 26 (3), 263–306, http://dx.doi.org/10.1016/0079-6611(91)90004-6.

Morel, A., Claustre, H., Antoine, D., Gentili, B., 2007. Natural variability of bio-optical properties in Case 1 waters: attenuation and reflectance within the visible and near-UV spectral domains, as observed in South Pacific and Mediterranean waters. Biogeosci. Discuss. 4 (4), 2147–2178.

Morel, A., Prieur, L., 1977. Analysis of variations in ocean color. Limnol. Oceanogr. 22 (4), 709–720.

Nagamani, P.V., Chauhan, P., Dwivedi, R.M., 2008. Development of chlorophyll *a* algorithm for Ocean Colour Monitor onboard OCEANSAT-2 satellite. IEEE Geosci. Remote Sens. Lett. 5 (3), 527–531, http://dx.doi.org/10.1109/LGRS.2008.923213.

Nair, V.E., Devassy, V.P., Madhupratap, M., 1992. Blooms of phytoplankton along the coast of India associated with nutrient enrichment and the response of zooplankton. In: Vollenweider, R.A., Marchetti, R., Viviani, R. (Eds.), Marine Coastal Eutrophication. Elsevier, Amsterdam, London, New York, Tokyo, 819–828.

O'Reilly, J.E., Maritorena, S., Mitchell, B.G., Siegel, D.A., Carder, K. L., Garver, S.A., Kahru, M., McClain, C.R., 1998. Ocean colour chlorophyll algorithms for SeaWiFS. J. Geophys. Res. 103 (C11), 24937–24953, http://dx.doi.org/10.1029/98JC02160.

O'Reilly, J.E., Maritorena, S., Siegel, D., O'Brien, M.C., Toole, D., Mitchell, B.G., et al., 2000. Ocean color chlorophyll *a* algorithms for SeaWiFS, OC2, and OC4: Version 4. In: Hooker, S.B., Firestone, E.R. (Eds.), SeaWiFS postlaunch technical report series. SeaWiFS post-launch calibration and validation analyses, Part 3, vol. 11 NASA/GSFC. 9–23.

Ouillon, S., Petrenko, A., 2005. Above-water measurements of reflectance and chlorophyll-*a* algorithms in the Gulf of Lions, NW Mediterranean Sea. Opt. Exp. 13 (7), 2531–2548, http://dx.doi.org/10.1364/OPEX.13.002531.

Pierson, D.C., Strombeck, N., 2000. A modelling approach to evaluate preliminary remote sensing algorithms: use of water quality data from Swedish Great Lakes. Geophysica 36 (1–2), 177–202.

Sathe, P.V., Jadhav, N., 2001. Retrieval of chlorophyll from the sea-leaving radiance in the Arabian Sea. J. Indian Soc. Remote Sens. 29 (1–2), 97–106.

Shanmugam, P., 2011. A new bio-optical algorithm for the remote sensing of algal blooms in complex ocean waters. J. Geophys. Res.-Oceans 116, C04016, http://dx.doi.org/10.1029/2010JC006796.

Siegal, D.A., Maritorena, S., Nelson, N.B., Hansel, D.A., Lorenzi-Kayser, M., 2002. Global distribution and dynamics of colored dissolved and detrital organic materials. J. Geophys. Res. 107, 3228, http://dx.doi.org/10.1029/2001JC000965.

Srinivas, K., Dineshkumar, P.K., 2006. Atmospheric forcing on the seasonal variability of sea level at Cochin, South west of India. Cont. Shelf Res. 26 (10), 1113–1133, http://dx.doi.org/10.1016/j.csr.2006.03.010.

Srinivas, K., Revichandran, C., Maheswaran, P.A., Ashraf, M.T.T., Murukesh, N., 2003. Propagation of tides in the Cochin estuarine system, South west coast of India. Indian J. Mar. Sci. 32 (1), 14–24.

Thomas, J.V., Premlal, P., Sreedevi, C., Kurup, M.B., 2004. Immediate effect of bottom trawling on the physicochemical parameters in the inshore waters (Cochin-Munambum) of Kerala. Indian J. Fish. 51 (3), 277–286.

Tilstone, G.H., Ingrid, M., Benavides, A., Pradhan, Y., Shutler, J.D., Groom, S., Sathyendranath, S., 2011. An assessment of chlorophyll-*a* algorithms available for SeaWiFS in coastal and open areas of the Bay of Bengal and Arabian Sea. Remote Sens. Environ. 115 (9), 2277—2291, http://dx.doi.org/10.1016/j.rse.2011.04.028.

Tilstone, G.H., Lotliker, A., Miller, P.I., Ashraf, P.M., Kumar, T.S., Suresh, T., Ragavan, B.R., Menon, H.B., 2013. Assessment of MODIS-Aqua chlorophyll *a* algorithms in coastal and shelf waters of the eastern Arabian Sea. Cont. Shelf Res. 65 (1), 14—26, http://dx.doi.org/10.1016/j.csr.2013.06.003.

Tzortziou, M., Subramaniam, A., Herman, J.R., Gallegos, C.L., Neale, P.J., Harding Jr., L.W., 2007. Remote sensing reflectance and inherent optical properties in the mid Chesapeake Bay. Estuar. Coast. Shelf Sci. 72 (1), 16—32, http://dx.doi.org/10.1016/j.ecss.2006.09.018.